

HANDOVER SCHEME FOR GSM BASED DEVICE-TO-DEVICE ULTRA DENSE NETWORKS

¹Dr.S.Prabakaran, ² Dr.R.Jegadeesan

^{1,2}Associate Professor, Dept. Of Computer Science & Engineering

^{1,2}Jyothishmathi Institute of Technology & Science, Karimnagar, India

Abstract: Internet of things (IoT) is expected to have billions of heterogeneously connected devices, demanding higher spectral efficiency, enhanced capacity and lesser latency. Device-to-Device (D2D) ultra-dense networks (UDN) are one of the potential components of 5G. Due to smaller cell sizes, more frequent handovers should be executed by the system. The devices should be always connected to the best network, while achieving seamless mobility. The handover failure leads to packet loss and degrades the quality of service (QoS). The unessential handover leads to wastage of resources. In this work, a vertical half handover (VHO) scheme is proposed for D2D-UDN. The proposed scheme dynamically selects two thresholds, which enables the system to maintain probability of VHO failure and probability of unessential handover below the desired bounds than the other conventional schemes.

IndexTerms-Device-to-Device (D2D), Heterogeneous networks (HetNet), Probability of unessential VHO, Probability of VHO failure, Ultra-dense networks (UDN).

I. INTRODUCTION

The increases in the number of devices (smart phones, tablets, etc.) tend to overload the core and access networks. The growth in data traffic over the years is displayed in Fig. 1 [1]. One of the major challenges experienced by telecom operators is huge traffic demand from evolved node B (eNB). The traffic offloading can be done by providing alternate paths to the loaded paths [2]. Third generation partnership project (3GPP) Release 12 discusses two offloading techniques like UDN and D2D communication [3]. D2D offloads traffic at both core and radio access networks. This enhances the network capacity. Small cells are also the efficient solution for traffic offloading [4]. The competition for resources decrease with the cell size becoming smaller over the generations. The deployment of more number of low power small cells results in UDNs. This enables frequency reuse and controls interference [5]. The different types of small cells defined in 3GPP Release 12 are listed in Table 1 [6].

Table 1. Comparison of 3GPP Release 12 small cells [6].

	Suitable environment	Deployment	Cell size	Capacity (Number of users supported)	Backhaul	Cost
Micro	Outdoor	Operator	250 m to 1 km	32 to 200	Operator	\$47,185
Pico	Hotspot	Operator	100 m to 300 m	32 to 64	Operator	\$13,865
Femto	Indoor	Consumer	10 m to 50 m	8 to 10	Consumer	\$100

Small cells along with D2D play a major role in offloading the traffic from eNB [7]. Small cells offload the hot spot traffic, whereas D2D offloads traffic for proximity services. In International mobile telecommunication standard (IMT-2020), this combination is expected to reduce delays and increase data rates within the networks [8]. D2D communication in UDNs and its applications are illustrated in Fig. 2. In Table 2, D2D is compared with the other short-range wireless transmission schemes [9].

The devices undergoing D2D communication may enter into the adjacent cells at some point. Due to this, the devices may not be in proximity. This may breakdown the connection between D2D devices and leading to a severe quality loss. Thus, handover in D2D communication is a challenging issue [10]. Handover in D2D is classified into half handover and joint handover [11].

When one of the devices in D2D communication moves away from the other device, the link between them may breakdown. To maintain seamless connectivity, one of devices is handed over to the neighboring network. This procedure is called half handover. These two devices are now connected by the cellular links. The process of half handover is explained in Figs. 3 and 4. When both the devices in D2D communication moves away from the current network, the link quality from the current network becomes weaker. To maintain call connectivity, both the devices are jointly handed over to the target network, which is termed as joint handover. A target network based handover selection method is proposed in [12] for composite radio environments. This algorithm uses received signal strength (RSS), required bit rate, delay, available system bandwidth and cost in decision making process. But the handover latency increases with the increase in available access points.

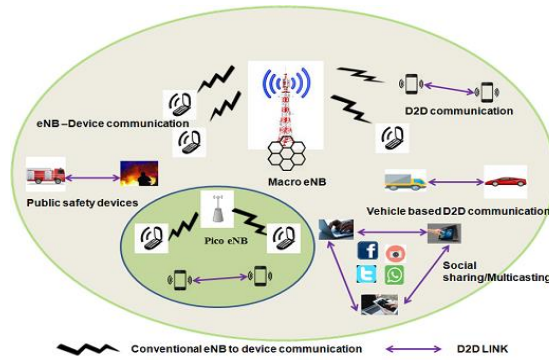


Fig. 2. D2D communication in UDNs and its applications.

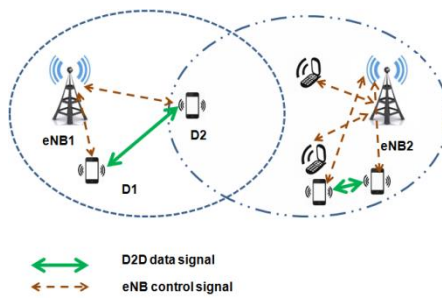


Fig. 3. Before half handover.

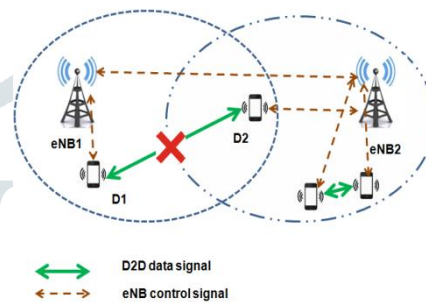


Fig. 4. After half handover.

Table 2. Comparison of short range wireless transmission techniques [9]

	Bluetooth 4.0	Near Field Communication (NFC)	WiFi Direct	Ultra wide band (UWB)	Zigbee	D2D
Standard	Blue tooth special interest group	ISO 13157	IEEE 802.11	IEEE 802.15.3a	IEEE 802.15.4	3GPP Release 12 Long Term Evolution Advanced (LTE-A)
Spectrum band	2.4 GHz	13.56 MHz	2.4 GHz, 5 GHz	3.1-10.6 GHz	868/915 MHz, 2.4 GHz	Licensed and Unlicensed
Maximum distance coverage	10-100m	0.2 m	200 m	10 m	10-100 m	10-1000 m
Peak data rate	25 Mb/s	424 Kb/s	250 Mb/s	480 Mb/s	250 Kb/s	5-10 Gb/s
Peer discovery	Require manual pairing	Discover by radio frequency	Need user settings for wireless access point	Require manual pairing	Network topology co-ordinator or Network ID broadcast	Device or eNB assisted
Fairness of service delivery	No	No	No	No	No	Yes

A markov based vertical handover (VHO) algorithm for HetNet is proposed in [13]. The handover decision is made based on network ID, bandwidth, delay, processing load and signaling overhead. This scheme is adaptive and suitable to varying environment and traffic conditions. But the implementation complexity is high.

A N-person cooperative game theory based bandwidth allocation scheme is proposed in [14] for 4G wireless networks. This scheme requires bandwidth and cost. This scheme efficiently manages the resources by providing VHO and new connections with the requested rate while maximizing their revenue. This scheme requires additional decision parameters to offer better QoS in practice.

In [15], a VHO scheme is proposed based on network QoS reputation. The network reputation is measured using a reputation system. This scheme also requires RSS and network load to make handover decisions. This scheme enables faster VHO decision. But the sustainability of the algorithm under varying traffic and environmental conditions are not addressed in this work.

Horrich et al. proposed a fuzzy logic based VHO algorithm in [16]. RSS, load and mobile velocity are given as the input for fuzzy inference engine (FIS). Based on the defuzzifier output, handover is executed. This scheme fails for varying traffic and environments. To enhance the performance further, a multi-layer perception neural network is used, which is getting trained by fuzzy input parameters and adapts them based on the environment and traffic variations.

An adaptive multi-objective VHO scheme for Hetnet is proposed in [17]. This scheme uses FIS and a modified Elman neural network (MENN) to make effective handover decisions. The bandwidth, device velocity and the number of users are given as the input for FIS. The complexity associated with fuzzy based approach is high when compared to other conventional approaches [16].The time complexity increases with the number of fuzzy inputs and rules. But all these schemes fails in maintaining probability of vertical handover failure and unessential handovers within bounds.

When the handover is timely triggered, unessential handover and handover failure can be avoided [18,19]. Yan X et al. [20] proposed a handover necessity estimation (HNE) scheme for a device entering a wireless local area network (WLAN) cell from a 3G cellular network. Based on the angle of arrival and angle of departure, the device travelling time in WLAN cell is estimated. Based on the distance thresholds, handover decision is made, which minimizes the probability of vertical handover failure and unessential handover. Here, the absolute difference between angle of arrival and angle of departure is in the range $[0, 2\pi]$.

Hussain R et al. [21] used a similar model, which considers difference angle in the range $[0, \pi]$. Here, distance thresholds are obtained using linear approximation. This shows significant improvement in maintaining probability of handover failure and unessential handover close to the desired bounds. In [22], dwell time is predicted using angle of arrival. The angle of arrival of the device into a WLAN is uniformly distributed between 0 and $\pi/2$. It has been proved that the thresholds measured using angle of arrival gives better control than schemes [20] and [21].In these schemes [20-23], the authors considered WLAN and 3G cellular networks for testing their proposed schemes.In this work, we use analytical models similar to the analytical models proposed in vertical handover necessity estimation [23] for testing half handover in D2D-UDN system.

The rest of the manuscript is organized in the following order: An analytical model to estimate the dwell time of Pico eNB is described in section 2. The analytical expressions for probability of VHO and probability of unessential handover are derived in section 3. In section 4, the parameters taken for simulation study and the results are elaborated. Section 5 concludes the paper by highlighting the future scope.

1. Dwell time estimation of Pico cell

Consider a D2D communication as in Fig. 5. The Macro eNB supports the control signals for the devices to communicate. Assume one of the device in D2D moves towards a Pico cell with constant velocity V m/s. It is assumed to take straight line motion within the Pico cell as indicated with dotted lines. To maintain high quality connection, half handover has to be executed, if necessary.

In Fig. 6, Pico cell is located at point E . y_{in} and y_{out} represent the device entry and exit points respectively. P is the middle point of the Pico cell straight line trajectory. I is the RSS sampling point, C is the coverage radius of Pico cell.

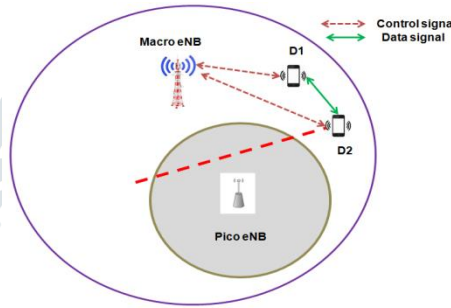


Fig. 5. Before half handover in D2D-UDN.

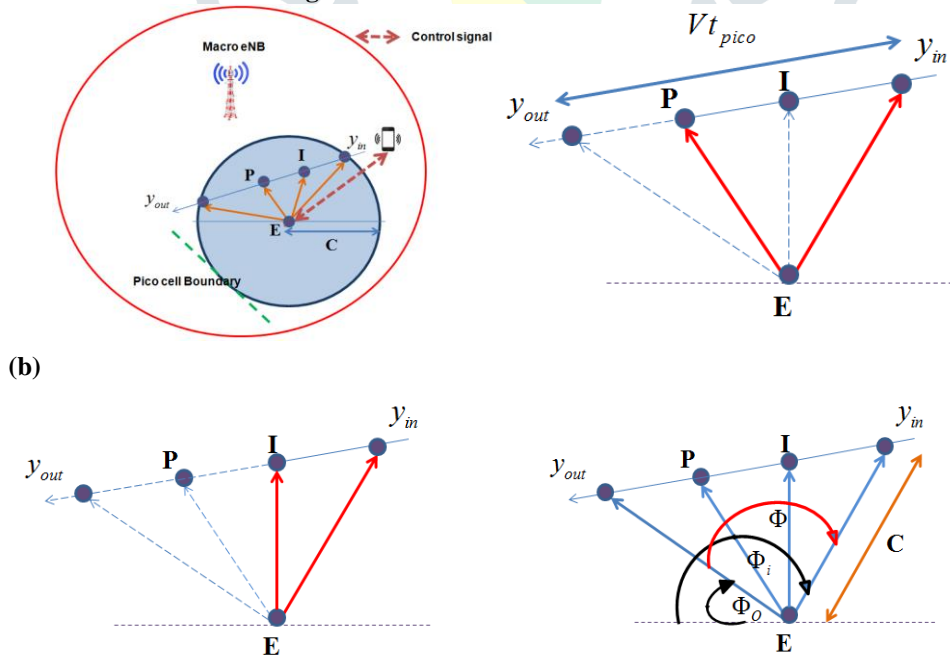


Fig. 6. Geometric representation of Pico cell in D2D-UDN.

The steps involved in predicting the dwell time of Pico cell are lined below. The Pico eNB coverage radius can be predicted using

$$C \square dE_{y_{in}} = d_o \cdot 10^{\frac{P_{tr} - P_o - RSS_{y_{in}}}{10\xi}} \quad (1)$$

where $dE_{y_{in}}$ is the distance between Pico eNB E and device entry point y_{in} , d_o is

the distance between E and reference point, P_{tr} is the transmit power of Pico eNB, P_o is the path loss at reference distance, $RSS_{y_{in}}$ is the RSS at the Pico cell entry point y_{in} , ξ is the path loss exponent. The distance between serving Pico eNB and RSS sampling point I is predicted using

$$d_{EI} = d_o \cdot 10^{\frac{P_{tr} - P_o - RSS_I}{10\xi}} \quad (2)$$

where d_{EI} is the distance between E and RSS sampling point I . The expressions (1) and (2) are derived from the log-normal shadowing path loss model [24]. From Fig. 6(b), the distance between points E and I is calculated using

$$(d_{EI})^2 = (d_{EP})^2 + (d_{y_{in}-P} - d_{y_{in}-I})^2 \quad (3)$$

where d_{EP} is the distance between points E and P , $d_{y_{in}-P}$ is distance between Pico cell entry point y_{in} and point P , $d_{y_{in}-I}$ is the distance between y_{in} and I .

Let the t_{pico} represents the dwell time i.e the time between the entry and exit points of Pico eNB. The distance covered in a Pico cell is given by Vt_{pico} . The distance between entry point and P is equivalently represented by

$$\frac{Vt_{pico}}{2} \quad (4)$$

The distance between entry point y_{in} and RSS sample point I is given by

$$d_{y_{in}-I} = V(t_I - t_{y_{in}}) \quad (5)$$

where t_I is the time taken to cross the Pico cell at point I , $t_{y_{in}}$ is the time at which the device entering at point y_{in} . From Fig. 6(c), we get

$$C^2 = (dE_{y_{in}})^2 = (d_{EP})^2 + (d_{y_{in}-P})^2 \quad (6)$$

By substituting (4) in (6), we get

$$C^2 = (d_{EP})^2 + \left(\frac{Vt_{pico}}{2}\right)^2 \quad (7)$$

By writing Eqs. (3) and (7) with respect to $(d_{EP})^2$ and equating results in dwell time, which is given by

$$t_{pico} = \frac{C^2 - d_{EI}^2 + V^2(t_I - t_{y_{in}})^2}{V^2(t_I - t_{y_{in}})^2} \quad (8)$$

Using (1) and (2), equation (8) can be rewritten as

$$t_{pico} = \frac{\left(d_o \cdot 10^{\left(\frac{P_{tr} - P_o - RSS_{y_{in}}}{10\xi}\right)}\right)^2 - \left(d_o \cdot 10^{\left(\frac{P_{tr} - P_o - RSS_I}{10\xi}\right)}\right)^2 + V^2(t_I - t_{y_{in}})^2}{V^2(t_I - t_{y_{in}})^2} \quad (9)$$

2. Threshold measurements

In this section, time threshold values for probability of VHO failure and unessential VHO are predicted to maintain these quantities within the desired bounds. The considered network environment with angle of arrival and angle of departure is illustrated in Fig. 6(d). The angles between the device entry and exit points of Pico eNB are ϕ_i and ϕ_o . These are uniformly distributed in $[0, 2\pi]$. The difference between the angles is represented by

$$\phi = |\phi_i - \phi_o| \quad (10)$$

The probability density function (pdf) associated with ϕ_i and ϕ_o are

$$f_{y_{in}(\Theta_i)} = \begin{cases} \frac{1}{2\pi}, & 0 \leq \Theta_i \leq 2\pi \\ 0, & \text{otherwise} \end{cases} \quad (11)$$

$$f_{y_{out}(\Theta_o)} = \begin{cases} \frac{1}{2\pi}, & 0 \leq \Theta_o \leq 2\pi \\ 0, & \text{otherwise} \end{cases} \quad (12)$$

The sites y_{in} and y_{out} are independent. Thus, the joint pdf associated is given by

$$f(\Theta_i, \Theta_o) = \begin{cases} \frac{1}{4\pi^2}, & 0 \leq \Theta_i, \Theta_o \leq 2\pi \\ 0, & \text{otherwise} \end{cases} \quad (13)$$

The cumulative distribution function (CDF) of ϕ can be measured using

$$F(\Theta) = P[\phi \leq \Theta] \quad (14)$$

The space site angles of entry and exit points of Pico eNB are $\phi \leq \Theta$ and $0 \leq \Theta \leq 2\pi$. Equation (14) can be rewritten using [23,25]

$$F(\Theta) = \frac{1}{4\pi^2} \left(\int_0^\Theta \int_0^{\Theta+\phi_1} + \int_\Theta^{2\pi-\Theta} \int_{\phi_1-\Theta}^{\Theta+\phi_1} + \int_{2\pi-\Theta}^{2\pi} \int_{\phi_1-\Theta}^{2\pi} \right) d\phi_o d\phi_i \quad (15)$$

This can be simplified as

$$F(\Theta) = \frac{1}{4\pi^2} [4\pi\Theta - \Theta^2], \quad 0 \leq \Theta \leq 2\pi \quad (16)$$

The pdf of Θ can be derived from (16), which is given by

$$f(\Theta) = \begin{cases} \frac{1}{\pi} \left(1 - \frac{\Theta}{2\pi}\right), & 0 \leq \Theta \leq 2\pi \\ 0, & \text{otherwise} \end{cases} \quad (17)$$

From Fig. 6(d), we get

$$t_{pico} \square g(\phi) = \sqrt{\frac{2C^2(1 - \cos\phi)}{V^2}} \quad (18)$$

The pdf of dwell time can be represented using fundamental theorem [26] as

$$f_T(t_{pico}) = \sum_{n=1}^2 \frac{f(\phi_n)}{|g'(\phi_n)|} \quad (19)$$

The first derivative of $g(\phi)$ is given by

$$g'(\phi_n) = \frac{C \sin\phi_n}{V \sqrt{2(1 - \cos\phi_n)}}, \quad n = 1, 2 \quad (20)$$

ϕ_1 and ϕ_2 can be obtained from (18), which are given as

$$\phi_1 = \arccos \left[1 - \frac{V^2 t_{pico}^2}{2C^2} \right] \quad (21)$$

where

$$\phi_2 = 2\pi - \phi_1 \quad (22)$$

$$\phi_2 = 2\pi - \arccos \left[1 - \frac{V^2 t_{pico}^2}{2C^2} \right] \quad (23)$$

Substituting the value of ϕ_1 in (20) yields

$$g'(\phi_1) = \frac{C \sin \left(\arccos \left(1 - \frac{V^2 t_{pico}^2}{2C^2} \right) \right)}{V \sqrt{2 \left(1 - \cos \left(\arccos \left(1 - \frac{V^2 t_{pico}^2}{2C^2} \right) \right) \right)}} \quad (24)$$

Simplifying (24) gives

$$|g'(\phi_1)| = \frac{C}{V} \sqrt{1 - \frac{V^2 t_{pico}^2}{4C^2}} \quad (25)$$

Substituting ϕ_2 in (20) yields

$$g'(\phi_2) = \frac{C \sin \left(2\pi - \arccos \left(1 - \frac{V^2 t_{pico}^2}{2C^2} \right) \right)}{V \sqrt{2 \left(1 - \cos \left(2\pi - \arccos \left(1 - \frac{V^2 t_{pico}^2}{2C^2} \right) \right) \right)}} \quad (26)$$

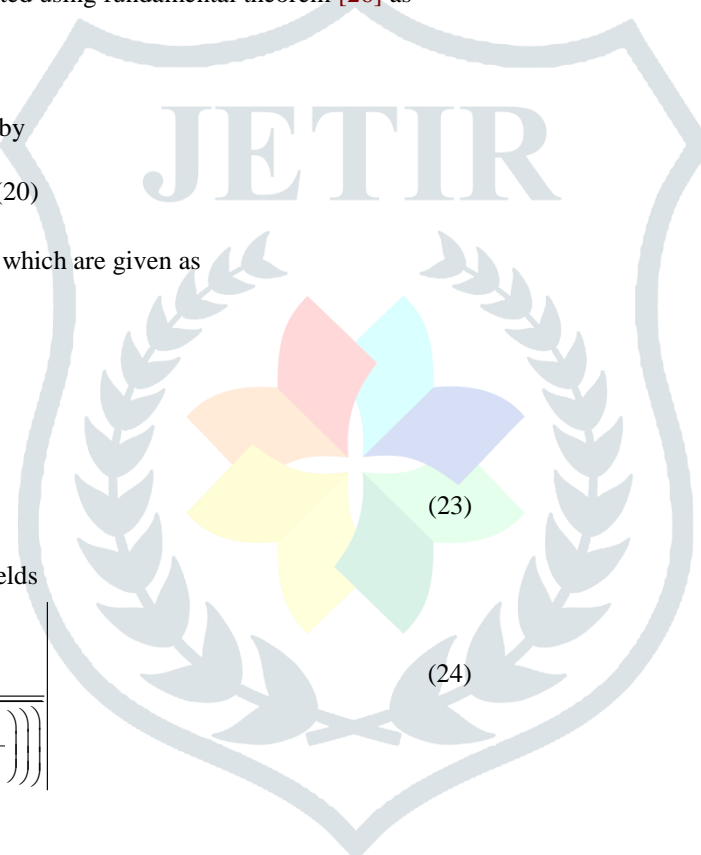
Simplifying (26) gives

$$|g'(\phi_2)| = \frac{C}{V} \sqrt{1 - \frac{V^2 t_{pico}^2}{4C^2}} \quad (27)$$

Substituting ϕ_1 and ϕ_2 values in (17) gives,

$$f(\phi_1) = \frac{1}{\pi} \left[1 - \frac{\arccos \left(1 - \frac{V^2 t_{pico}^2}{2C^2} \right)}{2\pi} \right] \quad (28)$$

$$f(\phi_2) = \frac{1}{\pi} \left[1 - \frac{2\pi - \arccos \left(1 - \frac{V^2 t_{pico}^2}{2C^2} \right)}{2\pi} \right] \quad (29)$$



By substituting (25), (27), (28) and (29) in (19), we get

$$f_T(t_{pico}) = \begin{cases} \frac{2V}{\pi\sqrt{4C^2 - V^2t_{pico}^2}}, & 0 \leq t_{pico} \leq \frac{2C}{V} \\ 0, & \text{otherwise} \end{cases} \quad (30)$$

To maintain handover failure and unessential handovers within bounds, two different time threshold values R and S corresponding to handover failure and unessential handovers are derived in this section.

3.1 Probability of VHO Failure

If the dwell time of Pico cell is less than handover latency from Macro cell to Pico cell (ζ_i), handover failure will occur. To maintain the handover failure within the limits, the handover is originated only when the predicted dwell time is greater than the time threshold (R) [22]. The probability of VHO failure is calculated using

$$P_{hf} = \int_R^{\zeta_i} f_T(t_{pico}) dt_{pico} \quad (31)$$

By substituting (30) in (31) and simplifying gives

$$P_{hf} = \begin{cases} \frac{2}{\pi} \left[\arcsin\left(\frac{V\zeta_i}{2C}\right) - \arcsin\left(\frac{VR}{2C}\right) \right], & 0 \leq R \leq \zeta_i \\ 0, & \zeta_i < R \end{cases} \quad (32)$$

The time threshold corresponding to VHO failure can be obtained from (32), which is given by

$$R = \frac{2C}{V} \sin \left[\arcsin\left(\frac{V\zeta_i}{2C}\right) - \frac{\pi P_{hf}}{2} \right] \quad (33)$$

3.2 Probability of Unessential VHO

If the sum of handover latency into ζ_i and out ζ_o of a Pico cell equals to the dwell time in a Pico cell, the device will not be able to use the Pico network resources at all. It has to initiate new handover again, once the previous moving in handover is completed. Here, the device unnecessarily uses the handover signalling without getting any benefit from the Pico network. To minimize unessential handovers, a handover into Pico cell is initiated only if the predicted dwell time is greater than time threshold S [22]. The probability of unessential handover is derived using

$$P_{uh} = \int_S^{(\zeta_i + \zeta_o)} f_T(t_{pico}) dt_{pico} \quad (34)$$

By substituting (30) in (34) and simplifying gives

$$P_{uh} = \begin{cases} \frac{2}{\pi} \left[\arcsin\left(\frac{V(\zeta_i + \zeta_o)}{2C}\right) - \arcsin\left(\frac{VS}{2C}\right) \right], & 0 \leq S \leq \zeta_i + \zeta_o \\ 0, & \zeta_i + \zeta_o < S \end{cases} \quad (35)$$

The time threshold corresponding to unessential VHO can be obtained from (35), which is given by

$$S = \frac{2C}{V} \sin \left[\arcsin\left(\frac{V(\zeta_i + \zeta_o)}{2C}\right) - \frac{\pi P_{uh}}{2} \right] \quad (36)$$

3. Simulation results and discussions

The parameters considered for simulation are listed in Table 3. Matlab 2017a simulation tool is used to validate the proposed work. The path loss models considered for Macro and Pico eNB are given by [6]

$$PL_{macro} (dB) = 128.1 + 37.6 \log_{10}(d) \quad (37)$$

$$PL_{pico} (dB) = 140.7 + 37.6 \log_{10}(d) \quad (38)$$

where d is the distance from serving node (Macro or Pico eNB) to the device. The scenario considered for simulation study is displayed in Fig. 7.

Table 3. Simulation settings.

Transmit power of Macro eNB	40 watts
Transmission power of Pico eNB	0.25 watts
Macro eNB coverage radius	3 km
Pico eNB coverage radius	0.25 km
Shadowing factor	6 dB
Minimum device speed	5 m/s
Additive white Gaussian noise(AWGN) Variance	-174 dBm/Hz
Handover latency	2 s
Service disruption time	1 s
Reference distance	1 m
Path loss exponent	3.5
Desired probability of VHO failure and unessential VHO	0.01 and 0.02

The entry and exit points of the device in a Pico cell is marked with labels y_{in} and y_{out} . The serving Macro and Pico eNBs are also marked in the Fig. 7. The dwell time of Pico cell with respect to velocity (m/s) is plotted in Fig. 8. It is clear that the increase in the velocity decreases the dwell time significantly. It also requires more frequent handovers.

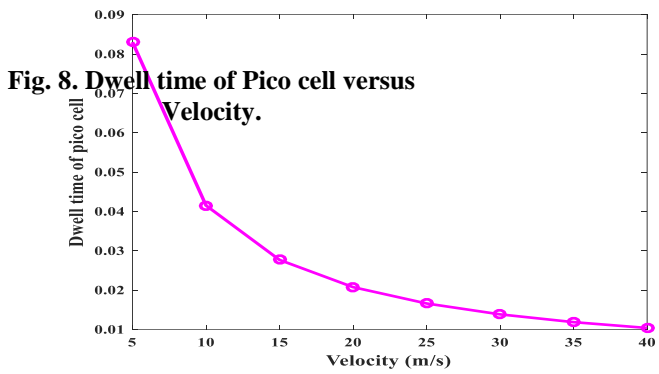
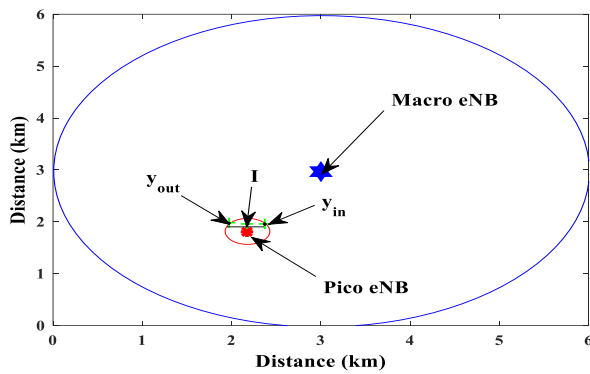


Fig. 7. Scenario considered for simulation.

Spectral efficiency gain is the number of additional bits per Hz that will be communicated if the device handovers to the new target network. The spectral efficiency gain due to VHO is given by [22]

$$SE_{gain} = (t_{pico} - t_{SI}) SE_{diff} - t_{SI} SE_{old} \tag{39}$$

where SE_{diff} is the spectral efficiency difference between the target and current network. t_{SI} is the service interruption time, SE_{old} is the spectral efficiency of current network.

The spectral efficiency difference between target and current network (b/s/Hz) versus spectral efficiency gain is compared for various velocities in Fig. 9. It is noted that the spectral efficiency gain decreases with the velocity. The increase in the spectral efficiency difference between target and current network increases the spectral efficiency gain. This figure is plotted by assuming the service interruption time as 1s.

In the VHO process, there is a time period for which the device is unable to transmit or receive any packets. This time period is called service interruption time. The increase in the service interruption time leads to larger packet loss and degrades the QoS. The spectral efficiency gain versus service interruption time is compared for different velocities in Fig.10. It is clear that the increase in the velocity, decreases the spectral efficiency gain.

The increase in the service interruption time increases the packet loss and thereby decreases spectral efficiency gain. This figure is plotted by assuming the spectral efficiency difference as 2b/s/Hz. Figs. 9 and 10 are plotted by assuming the spectral efficiency of current network as 5 b/s/Hz. We can make similar type of inference for the Figs. 11 and 12, which are plotted by assuming the spectral efficiency of current network as 10 b/s/Hz.

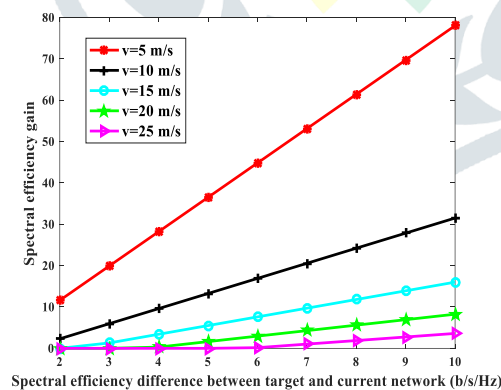


Fig. 9. Spectral efficiency gain versus spectral efficiency difference between target and current network for SE_{old} of 5 b/s/Hz.

In Fig. 13, the probability of VHO failure versus velocity is compared for different schemes with a desired probability of VHO failure bound of 0.01. Irrespective of the VHO schemes, probability of handover failure increases with the velocity. In Yan et al. [20] scheme, the probability of VHO failure deviates from the desired bound in a huge margin. In our proposed scheme, the probability of VHO failure gradually increases with the velocity.

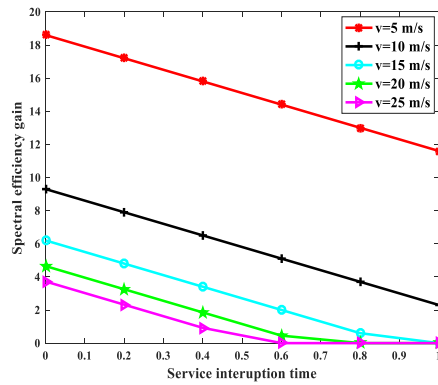


Fig. 10. Spectral efficiency gain versus service interruption time for SE_{old} of 5 b/s/Hz.

The process of obtaining the novel thresholds makes the achievable VHO failure probability closer to the desired bound. Our proposed scheme shows 24.37 % reduction in probability of VHO failure compared to the scheme proposed by Hussain et al. [21] for the velocity of 25 m/s.

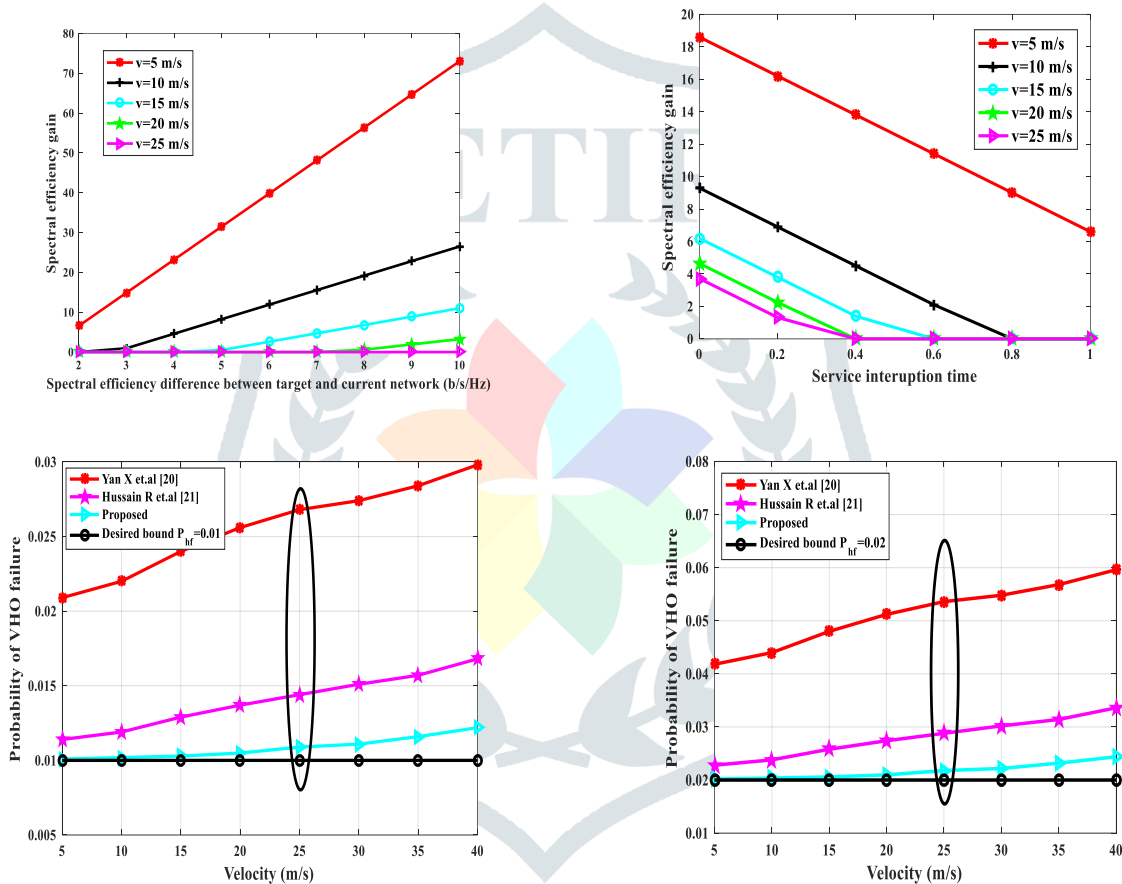


Fig. 13. Probability of VHO failure versus Velocity (m/s) for desired bound of 0.01.

In Fig. 14, the probability of VHO failure versus velocity is compared for different schemes with a desired probability of VHO failure bound of 0.02. The increase in the desired bound, increases the probability of VHO failure irrespective of the handover schemes. Our proposed scheme shows a significant performance even with the increase in desired bound.

In Fig. 15, the probability of unessential VHO versus velocity (m/s) is compared for different schemes with a desired probability of unessential VHO bound of 0.01. Irrespective of the VHO schemes, probability of unessential VHO increases with the velocity. In Yan X et al. [20] scheme, the probability of unessential VHO deviates from the desired bound in a huge margin. In our proposed scheme, the probability of unessential VHO gradually increases with the velocity. The process of obtaining the novel thresholds makes the achievable unessential VHO probability closer to the desired bound. Our proposed scheme shows 26.42 % reduction in probability of unessential VHO compared to scheme proposed by Hussain et al. [21] for the velocity of 25 m/s.

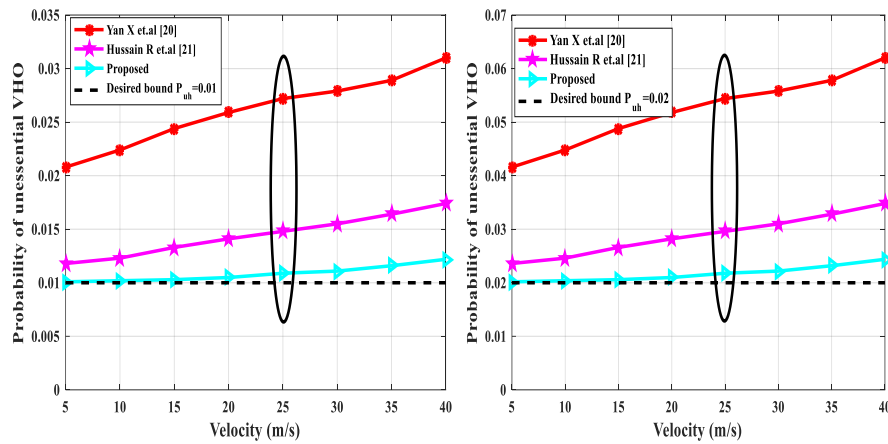


Fig. 14. Probability of VHO failure versus Velocity (m/s) for desired bound of 0.02.

Fig. 16. Probability of Unessential VHO versus Velocity (m/s) for desired bound of 0.02.

In Fig.16, the probability of unessential VHO versus velocity (m/s) is compared for different schemes with a desired probability of unessential VHO bound of 0.02. The increase in the desired bound increases the probability of unessential VHO irrespective of the handover schemes. Our proposed scheme shows a significant performance even with the increase in desired bound.

4. Conclusions

The proposed scheme first predicts the dwell time of the Pico cell. Based on the requirement, two thresholds values are dynamically chosen by the algorithm. Using these thresholds, the proposed VHO scheme enables the system to maintain probability of VHO failure and probability of unessential VHO within the required bounds. The simulation results prove that the proposed scheme is more suitable for heterogeneous environment. Irrespective of other schemes, the proposed scheme's probability of VHO failure and probability of unessential handover gradually increases with velocity and they are more closer to the required bounds. The promising results give route to further investigation on joint handover issues.

References

1. Index, C.V.N. (2013). The zettabyte era—trends and analysis. *Cisco white paper*.
2. Gandotra, P.; and Jha, R.K. (2016). Device-to-device communication in cellular networks: A survey. *Journal of Network and Computer Applications*, 71, 99-117.
3. Astely, D.; Dahlman, E.; Fodor, G.; Parkvall, S.; and Sachs, J. (2013). LTE release 12 and beyond. *IEEE Communications Magazine*, 51(7), 154-160.
4. Arthi, M.; Arulmozhivarman, P. (2016). A flexible and cost-effective heterogeneous network deployment scheme for beyond 4G. *Arabian Journal for Science and Engineering*, 41(12), 5093-5109.
5. Moon, S.; Bora K.; Saransh M.; Cheolwoo Y.; Huaping L.; Jeong-Ho K.; Jihyung K.; and Intae H. (2015). "Cell selection and resource allocation for interference management in a Macro-Picocell heterogeneous network." *Wireless Personal Communications* 83(3), 1887-1901.
6. Murugadass, A.; and Pachiyappan, A. (2017). Fuzzy Logic Based Coverage and Cost Effective Placement of Serving Nodes for 4G and Beyond Cellular Networks. *Wireless Communications and Mobile Computing*.
7. Malandrino, F.; Casetti, C.; and Chiasserini, C.F. (2014). Toward D2D-enhanced heterogeneous networks. *IEEE Communications Magazine*, 52(11), 94-100.
8. Baldemair, R.; Irnich, T.; Balachandran, K.; Dahlman, E.; Mildh, G.; Selén, Y.; and Osseiran, A. (2015). Ultra-dense networks in millimeter-wave frequencies. *IEEE Communications Magazine*, 53(1), 202-208.
9. Jegadeesan, R.; Sankar Ram, N. "Energy Consumption Power Aware Data Delivery in Wireless Network", Circuits and Systems, Scientific Research Publisher, 2016 (Annexure-I updated Journal 2016).
10. Chen, Q.; Zhang, Y.; and Tang, L. (2016). System Level Performance Evaluation for Ultra-Dense Networks. *Proceedings of International Conference of Communications and Networking in China*, Springer, Cham, 88-96.
11. Chen, H.Y.; Shih, M.J.; and Wei, H.Y. (2015). Handover mechanism for device-to-device communication. *Proceedings of IEEE Conference on Standards for Communications and Networking*, 72-77.
12. Ormond, O.; Perry, P.; and Murphy, J. (2005). Network selection decision in wireless heterogeneous networks. *16th IEEE international symposium Personal, indoor and Mobile Radio Communications*, 2680-2684.
13. Stevens-Navarro, E.; Wong, V.W.; and Lin, Y. (2007). A vertical handoff decision algorithm for heterogeneous wireless networks. *Proceedings of IEEE Wireless Communications and Networking Conference*, 3199-3204.
14. Niyato, D.; and Hossain, E. (2006). A cooperative game framework for bandwidth allocation in 4G heterogeneous wireless networks. *Proceedings of IEEE International Conference on Communications*, 4357-4362.
15. Zekri, M.; Jouaber, B.; and Zeglache, D. (2010). On the use of network QoS reputation for vertical handover decision making. In: *IEEE GLOBECOM Workshops*, 2006-2011.
16. Horrich, S.; Jamaa, S.B.; and Godlewski, P. (2007). Adaptive vertical mobility decision in heterogeneous networks. *Proceedings of IEEE Third International Conference on Wireless and Mobile Communication*, 44-44.

17. Guo, Q.; Zhu, J.; and Xu, X. (2005). An adaptive multi-criteria vertical handoff decision algorithm for radio heterogeneous network. *Proceedings of IEEE International Conference on Communications*, 2769-2773.
18. Yoo, S.J.; Cypher, D.; and Golmie, N. (2010). Timely effective handover mechanism in heterogeneous wireless networks. *Wireless Personal Communications*, 52(3), 449-475.
19. Kim, W.I.; Lee, B.J.; Song, J.S.; Shin, Y.S.; and Kim, Y.J. (2007). Ping-pong avoidance algorithm for vertical handover in wireless overlay networks. *Proceedings of IEEE Vehicular Technology Conference*, 1509-1512.
20. Yan, X.; Mani, N.; and Sekercioglu, Y.A. (2008). A traveling distance prediction based method to minimize unnecessary handovers from cellular networks to WLANs. *IEEE communications letters*, 12(1), 14-16.
21. Jegadeesan R, and Sankar Ram, N. "Energy-Efficient Wireless Network Communication with Priority Packet Based QoS Scheduling", *Asian Journal of Information Technology (AJIT)* 15(8): 1396-1404, 2016 ISSN: 1682-3915, Medwell Journal, 2016.
22. Hussain, R.; Malik, S.A.; Abrar, S.; Riaz, R.A.; Ahmed, H.; and Khan, S.A. (2013). Vertical handover necessity estimation based on a new dwell time prediction model for minimizing unnecessary handovers to a WLAN cell. *Wireless personal communications*, 71(2), 1217-1230.
23. Yan, X.; Sekercioglu, Y.A.; and Narayanan, S. (2010). *Optimization of vertical handover decision processes for fourth generation heterogeneous wireless networks*, PhD dissertation, Monash University.
24. R. Jegadeesan 1, Dr. N. Sankar Ram 2 October -2013 "ENROUTING TECHNIQUES USING DYNAMIC WIRELESS NETWORKS" *International Journal of Asia Pacific Journal of Research Ph.D Research Scholar 1, Supervisor 2, VOL -3 Page No: Print-ISSN-2320-5504*.
25. Jagannatham, A.K. (2015). *Principles of Modern Wireless Communication Systems* (1st ed.). McGraw-Hill Education.
26. Bettstetter, C.; Hartenstein, H.; and Pérez-Costa, X. (2004). Stochastic properties of the random waypoint mobility model. *Wireless Networks*, 10(5), 555-567.
27. Papoulis, A. (1965). *Probability, random variables, and stochastic processes* (1st ed.). McGraw-Hill Education.
28. Jegadeesan, R. Sankar Ram, and J. Abirmi "Implementing Online Driving License Renewal by Integration of Web Orchestration and Web Choreography" *International journal of Advanced Research trends in Engineering and Technology (IJARTET)* ISSN: 2394-3785 (Volume-5, Issue-1, January 2018)
29. Feng, D.; Lu, L.; Yuan-Wu, Y.; Li, G.Y.; Feng, G.; and Li, S. (2013). Device-to-device communications underlying cellular networks. *IEEE Transactions on Communications*, 61(8), 3541-3551.
30. Hussain, R.; Malik, S.A.; Abrar, S.; Riaz, R.A.; and Khan, S.A. (2012). Minimizing unnecessary handovers in a heterogeneous network environment. *Przegląd Elektrotechniczny*, 88(9b), 314-318

